15. J. Lippincott-Schwartz, J. Bonifacino, L. Yuan, R. Klausner, *Cell* **54**, 209 (1988).
16. B. Alarcon, B. Berkhout, J. Breitmeyer, C. Terhorst, *J. Biol. Chem.* **263**, 2953 (1988).
17. J. Bonifacino, C. Suzuki, J. Lippincott-Schwartz, A. Weissman, R. Klausner, *J. Cell Biol.* **109**, 73 (1989).
18. T. Wileman, G. Carson, J. Concino, A. Ahmed, C. Terhorst, *ibid.* **110**, 973 (1990).
19. C. Hall *et al.*, *Int. Immunol.* **3**, 359 (1991).
20. P. K. Srivastava, A. B. DeLeo, L. J. Old, *Proc. Natl. Acad. Sci. U.S.A.* **83**, 3407 (1986).
21. G. Koch, M. Smith, D. Macer, P. Webster, R. Mortara, *J. Cell Sci.* **86**, 217 (1986).
22. A. Mallabiabarrena, M. Fresno, B. Alarcon, *Nature* **357**, 593 (1992).
23. For immunofluorescence staining, cells were washed in phosphate-buffered saline (PBS), fixed in paraformaldehyde (3.7%) in PBS, permeabilized in cold methanol, and blocked in PBS containing goat serum (5%) and Triton X-100 (0.3%) (blocking buffer). Cells were then incubated with anti-calnexin in blocking buffer, washed in PBS, followed by incubation with fluorescein isothiocyanate (FITC)–conjugated goat antibody to mouse immunoglobulin G (IgG). Control double staining was done with lens culinaris lectin (E-Y Labs.) and anti–LAMP-1 [J. W. Chen *et al.*, *J. Cell Biol.* **101**, 85 (1985)]. Positive cells were examined on a Nikon Opti-phot 2 fluorescence microscope and photographed with Kodak T3200 film.
24. A 2-kb Spe I–Spe I fragment containing the coding region of calnexin was cloned into the Xba I site of expression vector Ap^{r}M8 (*6*) to generate the full-length calnexin construct. The RKPRRE-deleted calnexin cDNA was constructed by polymerase chain reaction (PCR) with the following oligonucleotide primers: 5′ primer, GGGGAATTCATGGAAGGGAAGTGG; 3′ primer, GGGAATTCTTAGTTTCTTGGTGATCTG. The CYT-deleted calnexin cDNA was also generated by PCR using the above 5′ primer with the following 3′ primer: GGAATTCTTATTCTTTCCAGAACAGCAG. Note that in the CYT-deleted calnexin, three anchor residues belonging to the cytoplasmic tail are present. After PCR amplification of the truncated calnexin cDNAs, the reaction products were digested with Eco RI and ligated into the Eco RI site of Ap^{r}M8 strain. DH5α-competent *Escherichia coli* were then transformed with the ligation products, and clones with correct inserts were used for transfections.
25. COS-7 cells were transfected by the DEAE-dextran method as described (*6*). Two days after transfection, cells were metabolically labeled for 5 hours with [^{35}S]methionine and [^{35}S]cysteine, lysed in 0.3% CHAPS lysis buffer, and immunoprecipitated as described (*6*).
26. S. Watkins, V. Raso, H. Slayter, *Histochem. J.* **22**, 507 (1991).
27. MOLT 13 cells were permeabilized with 8 μM digitonin, iodinated with lactoperoxidase, and solubilized in 1% digitonin in tris-buffered saline (TBS), and proteins were immunoprecipitated as described [F. Hochstenbach *et al.*, *J. Exp. Med.* **168**, 761 (1988)].
28. CD3ε cDNA [D. Gold *et al.*, *Nature* **321**, 431 (1986)] was ligated into the Eco RI site of the expression vector Ap^{r}M8. COS-7 cells were cotransfected with calnexin and CD3ε and permeabilized cells were stained as described (*23*). For double immunofluorescence analysis, cells were stained first with anti-CD3ε (SP34) and FITC-conjugated goat antibodies to mouse IgG. After blocking of the cells with isotype-matched myeloma MOPC 21 (Sigma), cells were stained either with AF8 or anti-gp96 (*20*) and then with the relevant rhodamine-conjugated secondary antibodies.
29. We thank D. Friend, L. B. Chen, and B. Brunkhorst for advice on immunofluorescence staining; H. Slayter for electron microscopy; and P. Srivastava, C. Terhorst, P. Anderson, and H. Ploegh for antibodies and cDNA clones. We also thank V. David, M. Sugita, C. Parker, and S. Porcelli for critically reading the manuscript. S.R. is a postdoctoral fellow of the Irvington Institute for Medical Research, and M.B.B. is a scholar of the Leukemia Society of America. Supported by grants from the National Institutes of Health.

13 September 1993; accepted 16 November 1993

Cell Membrane Resealing by a Vesicular Mechanism Similar to Neurotransmitter Release

Richard A. Steinhardt,* Guoqiang Bi, Janet M. Alderton

After injury to the cell membrane, rapid resealing of the membrane occurs with little loss of intracellular contents. This process has been studied by measurement of the rate of dye loss after membrane puncture in both the sea urchin embryo and 3T3 fibroblasts. Resealing of disrupted cell membranes requires external calcium that can be antagonized by magnesium. Block of multifunctional calcium/calmodulin kinase, which regulates exocytotic vesicle availability at synapses, and of kinesin, which is required for outward-directed transport of vesicles, inhibited membrane resealing. Resealing was also inhibited by botulinum neurotoxins B and A, suggesting that the two synaptosomal-associated proteins synaptobrevin and SNAP-25 also participate in resealing. This pattern of inhibition indicates that the calcium-dependent mechanisms for cell membrane resealing may involve vesicle delivery, docking, and fusion, similar to the exocytosis of neurotransmitters.

The resealing of plasma membranes is observed in experiments in which material is delivered to the cytoplasm by microinjection, chemical permeabilization, or electroporation (*1–5*). Indeed, it is not uncommon to observe rapid resealing of plasma membranes with little loss of intracellular contents. This property of cells must reflect the need to repair plasma membranes in the normal course of events experienced by cells. Transient plasma membrane disruptions commonly occur in cells that experience mechanical stress, such as gut, skin, endothelium, and muscle (*6–10*). Although erythrocytes will reseal and lipid bilayers can passively fuse together under some circumstances without Ca^{2+} (*11–15*), there is no evidence to suggest that similar passive processes are used by cells to repair their membranes. On the contrary, the fact that cells require Ca^{2+} to reseal (*3, 16–18*) suggested to us that an influx of Ca^{2+} might signal cell injury and trigger active mechanisms, similar to exocytosis, to rapidly seal membranes and ensure cell survival. We disrupted cell membranes by micropuncture with glass micropipettes and measured the resealing by observing the rate of fluorescent dye loss and monitoring the levels of free intracellular Ca^{2+} (*19*). We took advantage of the difference between unfertilized sea urchin eggs, with vesicles already docked in abundance at the plasma membrane, and the fertilized egg (embryo) in which docked vesicles had been depleted (*20*).

Department of Molecular and Cell Biology, University of California, Berkeley, CA 94720.

*To whom correspondence should be addressed.

In sea urchin eggs or embryos, which have a low surface to volume ratio, successful healing is rapid enough so that little or no dye loss is detected. In Swiss 3T3 cells the fraction of dye loss after micropuncture is a much larger fraction of the total and the wound to the plasma membrane involves a larger proportion of the surface. In 3T3 cells, therefore, it is easier to get more exact estimates of the time to reseal because a larger fraction of the dye is rapidly lost after micropuncture. Successful resealing required 10 to 30 s, but took longer when Ca^{2+} concentrations were low, as long as 90 to 120 s in some cases. We found threshold concentrations of Ca^{2+} in external solutions for plasma membrane resealing after micropuncture. Figure 1 illustrates examples of both successful resealing above the threshold Ca^{2+} requirement (Fig. 1A, embryo; Fig. 1C, fibroblast) and unsuccessful membrane repairs (Fig. 1B, embryo; Fig. 1D, fibroblast) below the threshold.

The threshold Ca^{2+} concentration, below which resealing did not take place, varied by cell type and cell state, and the concentration of Mg^{2+}. Unfertilized eggs in artificial seawater without Mg^{2+} healed at 300 μM Ca^{2+} and above (Fig. 2A). In artificial seawater with normal Mg^{2+} (55 mM), the threshold for healing was 1.2 to 1.3 mM Ca^{2+} (Fig. 2B). In 1 mM Mg^{2+} seawater the Ca^{2+} threshold was similar to that in 55 mM Mg^{2+} seawater, indicating a strong antagonism at low concentrations of Mg^{2+}. The state of the egg cortex determined the Ca^{2+} threshold for resealing. In fertilized eggs (embryos) or activated portions of egg surface, where the vesicles had already fused, the Ca^{2+} threshold was high-

er, 1.1 to 1.5 mM in zero Mg^{2+} (Fig. 2C) and 2.2 to 2.3 mM in 55 mM Mg^{2+} (Fig. 2D). Once the egg was fertilized, we did not observe any change in healing properties associated with that stage of the cell cycle. If only a portion of the surface had discharged its secretory vesicles, then that portion exhibits the higher Ca^{2+} threshold characteristic of the activated or fertilized egg, whereas the undischarged cortex continues to show the lower threshold. Swiss 3T3 cells exhibited Ca^{2+} thresholds for resealing in the range of 200 to 400 μM (Fig. 2E) in zero Mg^{2+} and showed antagonism by Mg^{2+} (Fig. 2F). Resealing in 3T3 cells was 100% at 0.8 mM Ca^{2+}, zero Mg^{2+} and less than 40% in 0.8 mM Ca^{2+}, 10 mM Mg^{2+}.

Neurotransmission has a similar Ca^{2+} requirement and is similarly inhibited by Mg^{2+}. The Ca^{2+} concentrations that we found for resealing are of similar magnitude as those required for a high probability of releasing 1 to 10 quanta to a single action potential (*21*, *22*). Intracellular Ca^{2+} concentration microdomains on the order of 200 to 300 μM exist against the cytoplasmic surface of the plasmalemma during transmitter secretion, supporting the view that the synaptic vesicular fusion for transmitter release is triggered by the activation of a low-affinity Ca^{2+}-binding site at the

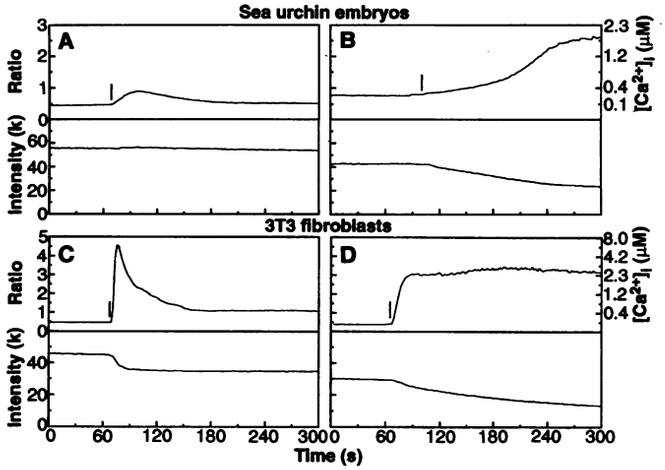

Fig. 1. Time course of membrane resealing in sea urchin embryos and 3T3 fibroblasts. Top traces in each experiment show intracellular free Ca^{2+} ($[Ca^{2+}]_i$) with fura-2, while bottom traces show the dye content of cells at a Ca^{2+}-insensitive function of excitation wavelength (*19*). Event mark indicates puncture. (**A**) *Lytechinus pictus* embryo responding to micropuncture and resealing in ASW (*19*). (**B**) *Lytechinus pictus* embryo failing to reseal in reduced Ca^{2+} after micropuncture in ASW at 2.2 mM Ca^{2+}. (**C**) Swiss 3T3 fibroblast responding to micropuncture and resealing in Puck's saline at 0.8 mM Ca^{2+}, zero Mg^{2+} (*19*). (**D**) Swiss 3T3 fibroblast failing to reseal in reduced Ca^{2+} after micropuncture in Puck's saline at 0.4 mM Ca^{2+}, 8 mM Mg^{2+}.

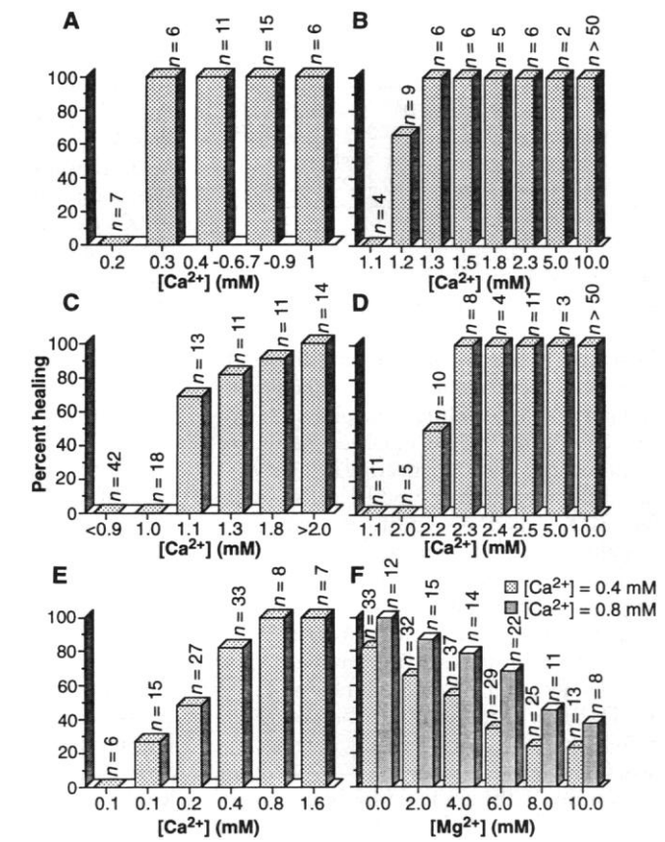

Fig. 2. External Ca^{2+} requirements and Mg^{2+} antagonism for membrane resealing after micropuncture; *n*, number of cells tested with micropuncture, one or more times. (**A**) Unfertilized eggs in zero Mg^{2+} ASW. (**B**) Unfertilized eggs in ASW. (**C**) Fertilized or activated eggs in zero Mg^{2+} ASW. (**D**) Fertilized or activated eggs in ASW. (**E**) 3T3 fibroblasts in zero Mg^{2+} Puck's saline. (**F**) 3T3 fibroblasts, in different levels of Mg^{2+}, in 0.4 mM and 0.8 mM Ca^{2+} Puck's saline.

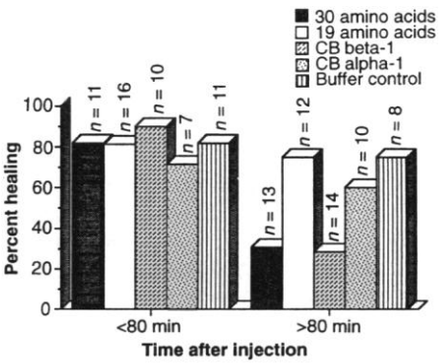

Fig. 3. Effect of CaM kinase reagents on membrane resealing after micropuncture in 3T3 fibroblasts. Microinjection solutions for all figures are described in (*19*).

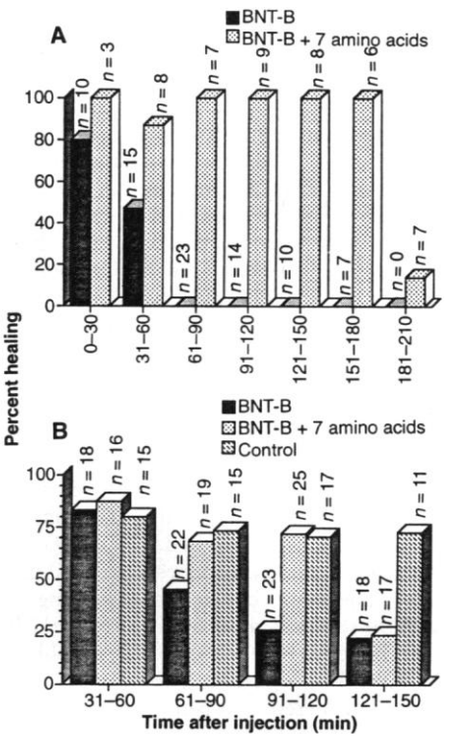

Fig. 4. Effect on plasma membrane resealing of botulinum neurotoxin B microinjected with and without the seven–amino acid peptide sequence around the Gln^{76}-Phe^{77} cleavage site (ASQFETS) of synaptobrevin-2 (*32*). (**A**) Fertilized eggs. (**B**) 3T3 fibroblasts. A, Ala; E, Glu; F, Phe; Q, Gln; S, Ser; and T, Thr.

active zone (*23*). These similarities in Ca^{2+} requirements and antagonism by Mg^{2+} led us to test for proteins previously hypothesized to control vesicle availability and function in exocytosis.

Multifunctional Ca^{2+}/calmodulin-dependent kinase (CaM kinase) is highly enriched at nerve terminals, both presynaptically and postsynaptically (*24*), and is associated with synaptic vesicles (*25*). CaM kinase may regulate the pool of available vesicles by phosphorylation of synapsin I and release of vesicles from actin-binding sites (*26, 27*). By using autoinhibitory peptide and an inhibitory antibody, we tested for a role of CaM kinase in plasma membrane resealing. Injection of a 30–amino acid portion of the regulatory domain of CaM kinase, which blocks CaM kinase activity in sea urchin embryos (*2*), into fertilized or activated eggs completely inhibits resealing to subsequent micropunctures (Table 1). A 19–amino acid portion from the regulatory domain did not have any effect, even in large excess (*2*). Antibody CB beta-1 to rat brain CaM kinase selectively precipitates CaM kinase from sea urchin homogenates and inhibits nuclear envelope breakdown (*2*). CB beta-1 injected into fertilized eggs blocked healing completely as soon as it was tested after injection (Table 2). Antibody CB alpha-1, which does not react with the sea urchin protein (*2*), had no effect on membrane resealing in these embryos. These results are consistent with those obtained on nuclear envelope breakdown in sea urchin embryos. The eggs all appear healthy, do not lose dye until the test micropuncture, and are blocked before nuclear envelope breakdown in the cell division cycle. Neither peptides nor antibodies had any effect on healing in unfertilized eggs whose secretory vesicles are already docked. The inhibitory 30–amino acid peptide and CB beta-1 were then tested for their effect on membrane resealing in Swiss 3T3 fibroblasts. In 3T3 cells, an initial injection (5 to 10% of the cell volume), even of buffer solution, was followed by an attenuation of healing, so that successful resealing occurred in 80% of the cells. The reagents against CaM kinase had no effects on subsequent micropunctures before 80 min after injection, but reduced healing to 20% of the cells after 80 min (Fig. 3). In this respect, 20% of the 3T3 fibroblasts behaved like unfertilized eggs, which may reflect a difference in cell state, related to vesicle availability, despite the fact that all tested cells were in interphase.

Kinesin is postulated to be the motor for outward-directed vesicle movement along cytoplasmic microtubules (*28*). The SUK-4 antibody to an adenosine triphosphate–sensitive microtubule-binding fragment of the 130-kD heavy chain of sea urchin kinesin blocks kinesin-driven motility (*29*). SUK-2 antibody to another site on the heavy chain has no effect on motility (*29*). We used these monoclonal antibodies to test for a role for kinesin in plasma membrane resealing. SUK-4 blocked resealing in fertilized eggs without affecting cell division and inhibited healing in 3T3 cells (Table 3). SUK-2 had no effect. As expected, resealing in unfertilized eggs was not inhibited, since vesicles were already in place at the plasma membrane.

Synaptobrevin-2 is an integral membrane protein present in small synaptic vesicles (*30, 31*). Botulinum neurotoxin B (BNT-B), an endopeptidase, blocks neurotransmission by cleaving synaptobrevin at a specific single site (*32*) after a delay for activation of the protease by reduction of an interchain disulfide bond (*33*). Injection of BNT-B blocked membrane healing in fertilized eggs without affecting healing in unfertilized eggs or cell division and reduced healing to 20% in Swiss 3T3 fibroblasts (Fig. 4). This block in membrane repair is delayed about 1 hour (Fig. 4), as is the block in neurotransmission (*32*). A 10,000-fold excess of a seven–amino acid peptide of the sequence around the Gln-Phe cleavage site will delay BNT-B block of neurotransmission for 1 hour or more (*32*). We coinjected BNT-B with this peptide (6,000 to 13,000 molar excess) and delayed the inhibitory effects for 2 to 3 hours in fertilized eggs and 1 to 2 hours in 3T3 fibroblasts (Fig. 4). Until recently the only protein known to contain this sequence was synaptobrevin-2 (*32*). A homologous protein, cellubrevin, has now been shown to be expressed in all tissues and cells tested and has the same cleavage site for BNT-B and tetanus-toxin protease (*33*). Coinjection of a 13,000-fold excess of another peptide (the 19–amino acid CaM kinase control peptide) with BNT-B did not delay block of resealing.

Botulinum neurotoxin A (BNT-A) inhibition of neurotransmitter release also requires time to develop, even when applied intracellularly (*34*). When purified BNT-A was injected, membrane healing was inhibited in both fertilized eggs and Swiss 3T3 cells (Table 4). Unfertilized eggs were not affected, as was the case with BNT-B. BNT-A acts as a protease that

Table 1. Healing in fertilized eggs of *L. pictus* injected with autoinhibitory and control peptides of CaM kinase. Autoinhibitory peptide does not block resealing during its microinjection. The block of resealing is complete by the time of first test micropuncture at 15 min after microinjection. Microinjection solutions for all tables are described in (*19*). N.A., not applicable.

Intracellular concentration (μM)	Percent healing (*n*)		
	Autoinhibitory 30–amino acid peptide	Control 19–amino acid peptide	Buffer only
0–19	50 (10)	N.A.	100 (6)
20–59	0 (6)	100 (3)	100 (8)
60–550	0 (1)	100 (10)	100 (6)

Table 2. Healing in fertilized eggs of *L. pictus* injected with antibodies to CaM kinase. Injections with low concentrations of antibody CB beta-1 do not inhibit healing immediately. Failure to heal begins about 45 min after injection for injection volumes 1 to 2% of egg volume. Higher concentrations of CB beta-1 block healing of the earliest wounds beginning about 15 min after injection.

Percentage of egg volume injected	Percent healing (*n*)	
	Antibody CB beta-1	Antibody CB alpha-1
1–4.9	0 (7)	100 (6)
5–11	0 (3)	100 (13)

Table 3. Healing in fertilized eggs of *L. pictus* and Swiss 3T3 fibroblasts injected with antibodies to kinesin.

Percentage of cell volume injected	Percent healing (*n*)		
	SUK-4	SUK-2	Buffer control
Fertilized eggs of L. pictus			
1.5–10	0 (23)	100 (14)	100 (9)
Swiss 3T3 fibroblasts			
5–10	21 (42)	74 (23)	79 (19)

Table 4. Effect of BNT-A on membrane healing in unfertilized sea urchin eggs, sea urchin embryos, and Swiss 3T3 fibroblasts.

Minutes after injection	Percent healing (*n*)
Unfertilized eggs of L. pictus	
20–130	100 (10)
150–240	100 (8)
Fertilized eggs of L. pictus	
20–130	100 (11)
150–240	0 (11)
Swiss 3T3 fibroblasts	
20–60	85 (13)
80–180	26 (27)

selectively cleaves the synaptic protein SNAP-25 (*35*). Thus, a second component of the putative fusion complex mediating synaptic vesicle exocytosis is implicated in plasma membrane resealing.

Our results showing differences between fertilized and unfertilized eggs suggest that membrane resealing may be designed to make quick use of secretory vesicles that normally have other uses (*20, 36*). The large secretory vesicles in unfertilized eggs can be seen directly by phase microscopy and were discharged quickly in unfertilized eggs at the site of a healed membrane rupture but slowly or not at all at sites that failed to heal in subthreshold Ca^{2+}. The similarities of membrane resealing with neurotransmission imply that features formerly thought to be specializations of the nervous system may be elaborations of a more fundamental cell survival mechanism, such as the placement of a voltage-gated Ca^{2+} "wound" next to the docking sites of an active zone. Therefore, some aspects of neurotransmission could be studied in cultured cell suspensions, independent of nervous system origin. Our results also suggest that the CaM kinase and kinesin reagents used here could be used to directly test their hypothesized role in maintaining the availability of synaptic vesicles (*26, 27, 37–40*). The specific mechanisms of inhibition by the clostridial neurotoxins imply that the fundamental process of plasma membrane resealing involves a membrane addition by exocytosis that may be the evolutionary ancestor to other membrane additions, such as Ca^{2+}-triggered secretion and neurotransmission.

REFERENCES AND NOTES

1. P. E. Tatham and B. D. Gomperts, *J. Cell Sci.* **98**, 217 (1991).
2. C. Baitinger, J. Alderton, M. Poenie, H. Schulman, R. A. Steinhardt, *J. Cell Biol.* **111**, 1763 (1990).
3. R. R. Swezey and D. Epel, *Cell Regul.* **1**, 65 (1989).
4. K. Hughes and N. Crawford, *Biochim. Biophys. Acta* **981**, 277 (1989).
5. C. el-Moatassim and G. R. Dubyak, *J. Biol. Chem.* **267**, 23664 (1992).
6. P. L. McNeil and S. Ito, *Gastroenterology* **96**, 1238 (1989).
7. ———, *J. Cell Sci.* **96**, 549 (1990).
8. P. L. McNeil, L. Muthukrishnan, E. Warder, P. A. D'Amore, *J. Cell Biol.* **109**, 811 (1989).
9. Q. C. Yu and P. L. McNeil, *Am. J. Pathol.* **141**, 1349 (1992).
10. P. L. McNeil and R. Khakee, *ibid.* **140**, 1097 (1992).
11. D. C. Chang and T. S. Reese, *Biophys. J.* **58**, 1 (1990).
12. N. J. Severs, A. M. Slade, T. Powell, V. W. Twist, C. R. Green, *J. Muscle Res. Cell Motil.* **11**, 154 (1990).
13. J. F. Hoffman, *Adv. Exp. Med. Biol.* **326**, 1 (1992).
14. B. Lee, K. McKenna, J. Bramhall, *Biochim. Biophys. Acta.* **815**, 128 (1985).
15. D. E. Leckband, C. A. Helm, J. Israelachvili, *Biochemistry* **32**, 1127 (1993).
16. W. C. de Mello, G. E. Motta, M. Chapeau, *Circ. Res.* **24**, 475 (1969).
17. V. Rehder, J. R. Jensen, S. B. Kater, *Neuroscience* **51**, 565 (1992).
18. X. Y. Xie and J. N. Barrett, *J. Neurosci.* **10**, 3257 (1991).
19. *Lytechinus pictus* sea urchins were from Marinus, Inc. (Long Beach, CA) and were handled as described (*2*). Swiss 3T3 cells were grown in Dulbecco's minimum essential medium plus 8% fetal bovine serum (FBS). The 3T3 cells were grown on glass cover slips for microscopic observation. Injection and subsequent observations were performed at 21°C on the stage of a Zeiss IM35 inverted microscope with a Nikon UV-F40x lens. Eggs were in artificial seawater (ASW). Orion 100 mM $CaCl_2$ (Orion Research, Boston) was used to make ASW and Ringer's of varying Ca^{2+} concentrations. $MgCl_2$ (4.9 M; Sigma) was used to vary Mg^{2+} concentration. Other seawater salts were from Fisher Scientific, Fair Lawn, NJ. ASW was 484 mM NaCl, 27 mM $MgCl_2$, 29 mM $MgSO_4$, 10 mM KCl, 2.5 mM $NaHCO_3$, 10 mM $CaCl_2$ (pH 8.0). Reduced Ca^{2+} and Mg^{2+} ASW were compensated osmotically with NaCl. During experiments, we maintained 3T3 cells with defined Ca^{2+} and Mg^{2+} concentrations by supplementing $CaCl_2$ and $MgCl_2$ into Ca^{2+}-free Puck's saline (University of California, San Francisco, Cell Culture Facility). The saline solution during injections had 1.6 mM Ca^{2+} and zero Mg^{2+}. Fura-2 (Molecular Probes, Eugene, OR) was introduced into the cells by either acetoxymethyl-ester loading (AM ester) or direct microinjection of the cell-impermeant fura-2 pentapotassium salt (fura-2 salt) together with other reagents into sea urchin eggs or 3T3 fibroblasts. Omega dot glass tubing was used to make injection pipettes, which were break-beveled to create tip diameters of 2 to 3 μM. For 3T3 fibroblasts, automated microinjection was performed with Eppendorf microinjector 5242 and micromanipulator 5170 (Eppendorf, Germany). Injection time was 0.3 to 0.5 s. Injected volume was 5 to 10% of the cell volume for 3T3 cells and 3 to 5% of cell volume for most egg injections. For fura-2 AM-ester loading of 3T3 cells, a 1 mM dye stock in dimethyl sulfoxide was mixed with an equal volume of Pluronic F-127 (Molecular Probes) before dilution to a final concentration of 1 μM in Puck's saline with 1.6 mM Ca^{2+} and 8% FBS. Cells were loaded at 21°C for 1 hour. Injection volume was estimated by measurement of total cell fluorescence increase at 510 nM (excitation at 357 nM) produced by the inclusion of fura-2 in the injection solution. Injection solutions were as follows: Fura-2 salt plus buffer injection solution was 5.4 mM fura-2 salt in aspartate buffer (AB), 100 mM potassium aspartate, 20 mM Hepes (pH 7.2). The CaM kinase 30–amino acid polypeptide was 16 mM in AB. For 3T3 cells the peptide was mixed 2:13:1 and for eggs 3:16:1 with AB and 27 mM fura-2 salt. The 19–amino acid control polypeptide was 20 mM in AB and then mixed 4:1 for eggs and 3:1 for 3T3 cells with 27 mM fura-2 salt in AB. CaM kinase antibodies were of unknown concentrations in ascites fluid, except that the control antibody was more than twice as concentrated as the blocking antibody. Each antibody was mixed 4:1 with 27 mM fura-2 salt in AB. SUK-4 was in phosphate-buffered saline (PBS) at 0.8 mg/ml, and SUK-2 was at 1.14 mg/ml, also in PBS. Each antibody was mixed 4:1 with 27 mM fura-2 salt in AB before injection. BNT-B (Wako Bioproducts, Richmond, VA) was at 1 mg/ml, about 1.5 μM, in 200 mM NaCl, 50 mM sodium acetate (pH 6.0). This was mixed 2:2:1 with AB and 27 mM fura-2 salt in AB. For experiments with the seven–amino acid polypeptide substrate of BNT-B to delay the action of the toxin, the solution was 2:2:1 BNT-B solution plus 20 mM seven–amino acid polypeptide substrate of BNT-B in AB plus 27 mM fura-2 salt in AB. Final intracellular concentration of the toxin was about 30 to 60 nM for injections of 5 to 10% of cell volume. The substrate to toxin ratio was about 13300:1. The BNT-B plus 19–amino acid control polypeptide injection solution was 2:2:1 BNT-B solution plus 20 mM 19–amino acid CaM kinase polypeptide in AB plus 27 mM fura-2 salt in AB. BNT-B buffer-only control injection solution was 4:1 for eggs and 2:1 for 3T3 cells BNT-B buffer plus 27 mM fura-2 salt in AB. For injection of BNT-A, five parts pure toxin, free of hemagglutinin, obtained from B. R. DasGupta (1 mg/ml in AB), were mixed with one part 27 mM fura-2 salt in AB. For wounding, 1-mm-diameter glass tubing was pulled to make unbeveled wounding pipettes. For eggs, the pipette was advanced at a 35° angle from the stage toward the egg to create a dipple about 20% of the egg diameter deep. A tap was applied to the micromanipulator to wound the egg. After wounding, the pipette was withdrawn. Wounding of 3T3 cells used the same automated system as for microinjection. The time setting for wounding was 0.3 s. Wounding and healing were monitored by photometric measurement of fura-2 fluorescence at 510-nm excited with 357- and 385-nm light. The 357-nm excited fluorescent intensity was relatively insensitive to Ca^{2+} (6% increase for an increase of free Ca^{2+} from 100 nM to 1000 nM). The ratio of fluorescent intensity excited by 357- and 385-nm ultraviolet light was used to calculate intracellular Ca^{2+} concentration [R. Y. Tsien, T. J. Rink, M. Poenie, *Cell Calcium* **6**, 145 (1985)]. In Fig. 1, the intensity (from 357-nm excitation) was further modified by addition of a small fraction of 385-nm excited intensity (5%) and became insensitive to Ca^{2+}.
20. V. D. Vacquier, *Dev. Biol.* **84**, 1 (1981).
21. J. I. Hubbard, S. F. Jones, E. M. Landau, *J. Physiol. (London)* **196**, 75 (1968).
22. A. C. Crawford, *ibid.* **240**, 255 (1974).
23. R. Llinás, M. Sugimori, R. B. Silver, *Science* **256**, 677 (1992).
24. P. I. Hanson and H. Schulman, *Annu. Rev. Biochem.* **61**, 559 (1992).
25. P. Greengard, F. Valtorta, A. J. Czernik, F. Benfenati, *Science* **259**, 780 (1993).
26. R. Llinás, J. A. Gruner, M. Sugimori, T. L. McGuinness, P. Greengard, *J. Physiol. (London)* **436**, 257 (1991).
27. F. Benfenati *et al.*, *Nature* **359**, 417 (1992).
28. R. D. Vale, F. Malik, D. Brown, *J. Cell Biol.* **119**, 1589 (1992).
29. A. L. Ingold, S. A. Cohn, J. M. Scholey, *ibid.* **107**, 2657 (1988).
30. T. J. Südhof, M. Bauaat, M. S. Perin, R. Jahn, *Neuron* **2**, 1475 (1989).
31. M. Bauaat, P. R. Maycox, F. Navone, P. De Camilli, R. Jahn, *EMBO J.* **8**, 379 (1989).
32. G. Schiavo *et al.*, *Nature* **359**, 832 (1992).
33. H. T. McMahon *et al.*, *ibid.* **364**, 346 (1993).
34. B. Poulain *et al.*, *Proc. Natl. Acad. Sci. U.S.A.* **85**, 4090 (1988).
35. J. Blasi *et al.*, *Nature* **365**, 160 (1993).
36. B. M. Shapiro, *Science* **252**, 533 (1991).
37. M. P. Sheetz, E. R. Steuer, T. A. Schroer, *Trends Neurosci.* **12**, 474 (1989).
38. M. Gho, K. McDonald, B. Ganetzky, W. M. Saxton, *Science* **258**, 313 (1992).
39. A. Ferreira, J. Niclas, R. D. Vale, G. Banker, K. S. Kosik, *J. Cell Biol.* **117**, 595 (1992).
40. D. H. Hall and E. M. Hedgecock, *Cell* **65**, 837 (1991).
41. Peptides were synthesized by the Microchemical Facility, Cancer Research Laboratory, University of California, Berkeley, purified by high-pressure liquid chromatography, and confirmed by sequencing or mass spectroscopy.

We thank H. Schulman for CaM kinase antibodies, J. Scholey for kinesin antibodies, B. R. DasGupta for BNT-A, and J. Younger for comments on the manuscript. Supported by NIH National Institute of Arthritis and Musculoskeletal and Skin Diseases grant R01 AR41129.

22 July 1993; accepted 16 November 1993